Rapid Communications

# Bubble formation in freezing droplets

Fuqiang Chu,[1] Xuan Zhang,[2] Shaokang Li,[1] Haichuan Jin,[1] Jun Zhang,[1]
Xiaomin Wu,[2] and Dongsheng Wen[1,3,*]

[1]*School of Aeronautic Science and Engineering, Beihang University, Beijing 100191, China*
[2]*Department of Energy and Power Engineering, Tsinghua University, Beijing 100084, China*
[3]*School of Chemical and Process Engineering, University of Leeds, Leeds LS2 9JT, United Kingdom*

(Received 24 January 2019; published 23 July 2019)

Water droplet icing on solid surfaces has been intensively studied in recent years but still with many mechanisms unrevealed. Here, we report a bubble formation phenomenon that always occurs in freezing droplets, from millimeter-sized sessile droplets to microscale condensed droplets, during icing and condensation frosting. In the second stage of icing (the first stage is nucleation and recalescence), air dissolved in liquid water is separated out in the ice front, forming many isolated bubbles. Coupled with the droplet icing physics, a theoretical model was proposed to predict the bubble formation and elucidate its influencing factors. Due to the bubble formation, the final ice droplet is actually a porous medium, rather than a complete solid ice. These results bring new insight into icing physics, helping modify icing models and improve anti-icing and deicing techniques.

DOI: 10.1103/PhysRevFluids.4.071601

The icing phenomenon is ubiquitous in nature and industry. When the ambient temperature is below the freezing point, icing of a water droplet occurs. In most instances, icing is undesired and causes numerous problems, such as reduction of crop production in agriculture [1], reduction of lifting force with decreased flight safety in aviation [2], and heat transfer deterioration in heat exchanger systems [3]. Understanding the icing mechanisms and employing appropriate anti-icing technologies have been intensively studied in a few decades. Some progress have been made regarding the ice nucleation physics under humidity or gas flow environments [4,5], the freezing front growth and droplet shape evolution features [6–8], and the pointy tip formation mechanism at the later stage of icing [9,10]. Some unique phenomena or behaviors during icing have been investigated such as frost halo [11], dry zone [12], droplet trampolining [13], and droplet fragmentation and bursting [14,15]. A variety of anti-icing methods are also proposed to suppress the ice accretion, one of which is the application of nanoengineered surfaces [16]. Different surfaces with varied microstructures and wettability have been used to delay ice nucleation [17–19], reduce ice adhesion [20,21], and even self-clean supercooled droplets or melting frost [22–24].

In all of these studies, frozen ice has been considered as a tight solid, which may not be always true. It has been observed from ice disks [25], natural pond ice [26], and ice cubes frozen in fridges [27], that some bubbles may be formed. For sessile droplets, there was also some incidental observation that bubbles might form in ice beads [9,28]; for example, one can see the bubbles in two-dimensional (2D) freezing droplets captured by Marin *et al.* (although they do not mention the bubble formation in their Letter) [9]. However, nobody really embarks on research and attaches importance to the bubble formation in a freezing droplet, which is of great significance for anti-icing applications. Coupled with the peculiarity of the droplet icing dynamics, the accompanied bubble

*Corresponding author: d.wen@buaa.edu.cn

 

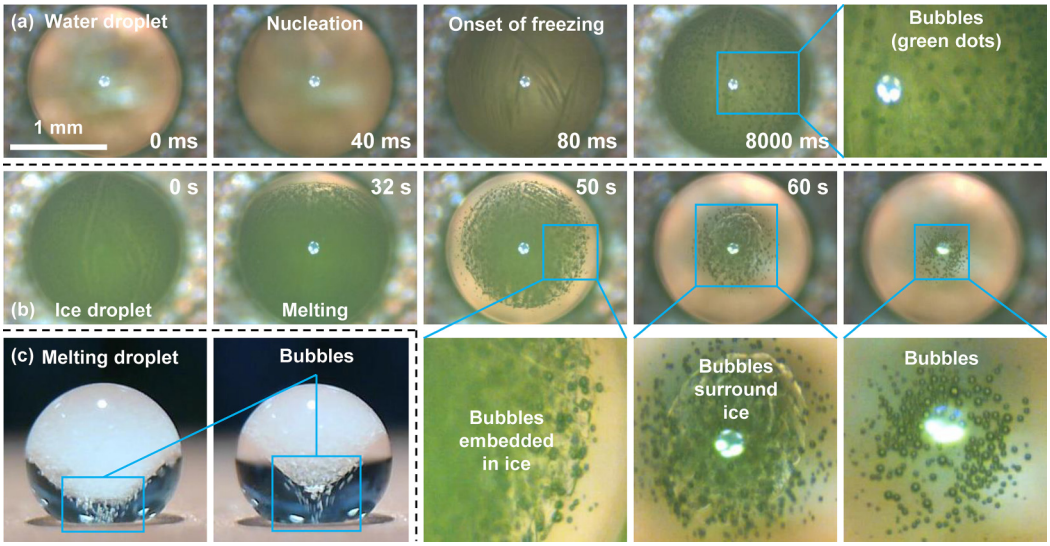


FIG. 1. (a) Direct observation of bubble formation during freezing of a sessile droplet from top view. In the second stage of icing, bubbles constantly appear. These bubbles are of micron scale. The partial enlarged drawing shows these bubbles more clearly. (b) Proof of bubble formation in freezing droplets via observing its melting process of an ice droplet from top view. From the partial enlarged drawings, one can see many tiny bubbles surrounding or embedded in the unmelted ice cover. (c) Proof of bubble formation in freezing droplets via observing the melting process from side view with many bubbles moving quickly from the unmelted ice cover.

formation becomes more complicated, and is affected by more factors compared with that in bulk ice such as ice disks. In this Rapid Communication, we demonstrate that the bubble formation phenomenon is common in icing droplets, regardless of the millimeter sessile droplets or microscale condensed droplets, and also independent of the surface characteristics. A theoretical model coupled with the droplet freezing physics was then proposed (also validated) to elucidate the relationship between the bubble formation and its influencing factors.

In this work, three aluminum-based surfaces (surfaces S1, S2, and S3) were used as the experimental surfaces. Both S1 and S2 are superhydrophobic at room temperature (20 °C), but when the test droplets are supercooled under icing conditions, the two surface contact angles (CAs) decrease. Surface S3 is hydrophilic. Then we conducted icing experiments and condensation frosting experiments. In the icing experiments, we used supercooled millimeter sessile droplets (deionized water without degas processing) of 1, 2, and 4 $\mu$l volume; while in the condensation frosting experiments, the condensed droplets are microscale with various sizes. During the experiments, the laboratory temperature was measured to be $20.0 \pm 1.0$ °C with a relative humidity range from 20% to 40%. The supercooled droplet temperatures were $-20.0 \pm 0.1$ °C on surface S1 and $-15.0 \pm 0.1$ °C on surface S2 and S3. See the detailed experimental section in the Supplemental Material [29].

Icing of a droplet usually experiences two stages including nucleation and recalescence (the nucleation is the starting point of the recalescence and the recalescence takes place quickly, during which the supercooling drives rapid kinetic crystal growths) and freezing (ice front growth), where the former is a rapid kinetically controlled process, and the latter is a heat transfer controlled process [4,6]. Figure 1(a) shows a top view of a typical icing phenomenon of a sessile droplet (2 $\mu$l droplet on S1), where one can see the nucleation and recalescence and the onset of freezing very clearly. However, it is found that many tiny bubbles begin to appear after the onset of freezing. As the ice front moves upward quickly, more and more bubbles are formed and some old bubbles are becoming

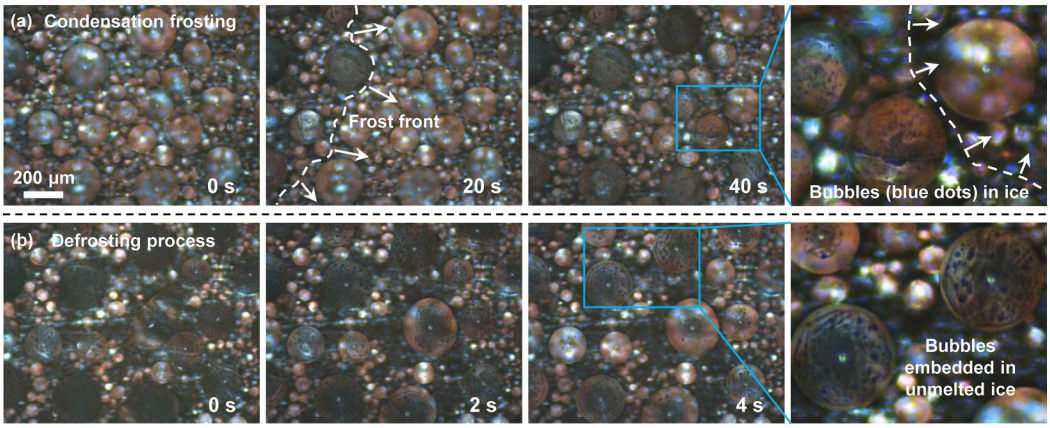


FIG. 2. (a) Direct observation of bubble formation in freezing droplets during condensation frosting. From the partial enlarged drawing, one can see the differences between the ice droplets behind the frost front and the water droplet ahead. Those tiny, dark-blue dots are bubbles entrapped in ice droplets. (b) Proof of bubble formation in freezing droplets during condensation frosting via observing the defrosting process. The partial enlarged drawing shows clearly that there are many bubbles (blue dots) embedded in the unmelted ice covers of droplets.

trapped inside the ice. After complete freezing of the droplet, there are clear dense spots distributed on and in the top-view droplet (see Supplemental Material video S1 [29]). These spots are trapped bubbles whose size is of 10 $\mu$m scale. To confirm this, Fig. 1(b) shows the deicing process of the ice droplet in Fig. 1(a). From the partial enlarged drawings, one can see clearly many tiny bubbles surrounding or embedded in the unmelted ice cover. Even when the ice melts completely, these bubbles exist for a period before dissolved into water again (see Supplemental Material video S2 [29]). The side-view images in Fig. 1(c) also clearly show the fast-moving bubbles around the unmelted ice cover (see Supplemental Material video S3 [29]). These images in Figs. 1(b) and 1(c) provide strong evidence of bubble formation in icing droplets.

Bubble formation not only exists in the freezing process of millimeter sessile droplets, but also occurs in microscale condensed droplets during condensation frosting. Figure 2(a) shows the condensation frosting process on surface S1 (see Supplemental Material video S4 [29]). From the partial enlarged drawing, one can see the differences between the ice droplets behind the frost front and the water droplet ahead. There are entrapped bubbles (dark-blue dots in the images) in the ice droplets, while the water droplets are limpid. Similarly, observing the defrosting droplets shown in Fig. 2(b), the bubbles embedded in the unmelted ice are also strong proof of the bubble formation in freezing droplets during condensation frosting (see Supplemental Material video S5 [29]).

In the experiments, we have observed the bubble formation in freezing droplets from microscale (a minimum droplet radius of 50 $\mu$m) to millimeter scale [a maximum droplet radius of 1 mm (4 $\mu$l volume)] on three surfaces with different microstructures and wettability (see the bubble formation in freezing droplets on surfaces S2 and S3 in Supplemental Material [29]). We conclude that the bubble formation phenomenon is common in microscale and larger freezing droplets, and independent of the surface characteristics. Bubble formation may also exist in the icing process of impacting droplets [30]. It is well known that water can dissolve a certain volume of air (i.e., 0 °C water has a saturated air solubility of about 3% volume fraction). Because the ice cannot match with the air in the crystal lattices, when the water solidifies into ice, the dissolved air has to dissolve out, forming bubbles in solid ice. However, one may ask if the bubble formation is purely due to the originally dissolved gas in water as we did not use degassed water to produce sessile droplets. To elucidate this query, the bubble formation in condensed droplets has provided the explanation. These condensate droplets do not have any gas inside when they are originally condensed; however, as long

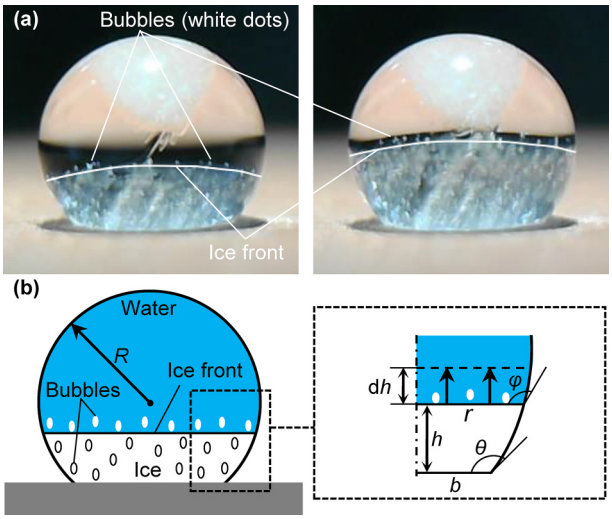


FIG. 3. (a) Bubble formation mechanism determination through a controlled reicing process of a partially melted ice droplet. One can see bubbles constantly separated out in the ice front. (b) Schematic of bubble formation in freezing droplets. $h$ is the ice front height, $dh$ is the moving distance of the ice front during $dt$ time, $r$ is the ice front radius, and $\varphi$ is the contact angle at the ice-water-gas triple line; $R$ is the droplet curvature radius, $b$ is the droplet base radius, and $b = R\sin\theta$, where $\theta$ is the surface contact angle.

as the droplet is in the air, it will dissolve the air. According to the Fick's law, the timescale for the air to dissolve in microcondensed droplets to saturation is $\sim$1 s, which is an order of magnitude shorter than that of the ice bridge growth during condensation frosting [22]. In other words, the condensed droplets have enough time to dissolve air to saturation, and the air will dissolve out in the freezing process.

To observe the bubble formation in icing droplets more clearly, we performed a reicing process, which means refreezing a partially melted ice droplet before the ice in the droplet melts completely. As mentioned above, the first stage of a pure water droplet icing is nucleation and recalescence, which could make the droplet appear cloudy [4]. As a result, it is hard to see how the bubble forms in an icing droplet. However, the reicing process is different. Because of the existence of ice, the reicing process does not experience the clouded recalescence stage, so the droplet remains transparent in the freezing stage. Figure 3(a) shows two images during the reicing process. One can see the ice front clearly, as well as the bubbles separated out from the ice front (see Supplemental Material video S6 [29]). Under our current experimental conditions, the calculated rising speed of bubbles (steady speed, $2\rho_{\text{water}}g{r_{\text{b}}}^2/9\eta_{\text{water}}$, where $r_{\text{b}}$ is the bubble radius, $\rho_{\text{water}}$ is the water density, and $\eta_{\text{water}}$ is the dynamic viscosity of water) based on the Stokes' law [31] is always smaller than the ice front speed, so old bubbles are trapped in ice before they could float up and new bubbles constantly form, until the droplet is frozen completely. But if the experimental droplet is large enough or the supercooling degree is small enough, some bubbles would escape the pursuit of the ice front and finally spill into the surrounding air.

To assess the bubble formation rate and determine its influencing factors, a theoretical model coupled with the droplet icing physics was proposed. In the model, we assume that the ice front is flat, and the bubbles are incompressible and will not evade into the surrounding air (i.e., the bubble volume is conservative). Water evaporation during icing is neglected to keep the water volume conservative. As shown in Fig. 3(b), after infinitesimal time, $dt$, the ice front moves up, $dh$, then solidified water volume, $dV_{\text{water}}$, is calculated as

$$dV_{\text{water}} = \nu(1-\beta)\pi r^2 dh, \tag{1}$$

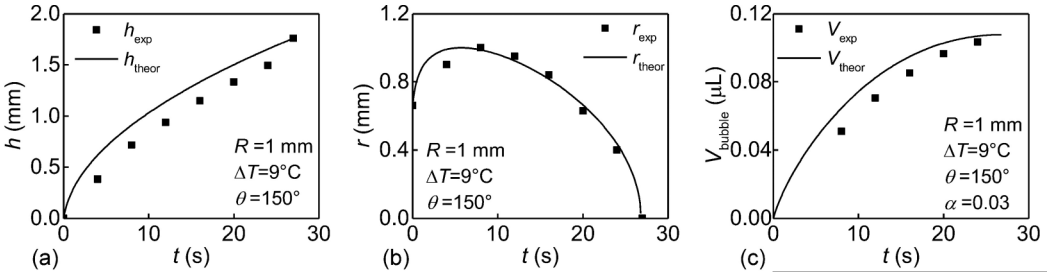


FIG. 4. (a) Variation of ice front height. We extracted the experimental results from the experiments by Marin *et al.* [9] and obtained the theoretical results by integrating Eq. (3). (b) Variation of ice front radius. The experimental results are from the experiments by Marin *et al.* [9] and the theoretical results are from Eq. (5). (c) Variation of bubble volume. For the experimental results, we obtained a 2D bubble area by processing the images captured by Marin *et al.* [9] and then transformed the 2D bubble area to 3D bubble volume through a mathematical process, while the theoretical bubble volume is an integration of Eq. (6).

where $\nu$ is the ratio of ice and water densities and $\beta$ is the bubble volume fraction in ice (assuming $\beta$ is constant everywhere). Considering the conservation of water and bubble volumes, bubble volume fraction, $\beta$, has a relation with the air solubility in water, $\alpha$. That is, $\alpha = \beta/[\nu(1-\beta)]$. So, the released bubble volume during $dt$ time is written as

$$dV_{\text{bubble}} = \left(1 + \frac{1}{\alpha\nu}\right)^{-1} \pi r^2 dh. \tag{2}$$

When assuming the ice front is flat (Stefan problem [32,33]), the relationship between the ice front height, $h$, and the time, $t$, can be derived as $h = (2\text{St Dt})^{0.5}$ [34], where St is the Stefan number, $\text{St} = Cp\Delta T/L_{\text{m}}$; $D$ is the thermal diffusivity, $D = \lambda_{\text{ice}}/(\rho_{\text{ice}} Cp)$. $\Delta T$ is the supercooled temperature; $Cp$, $\lambda_{\text{ice}}$, and $\rho_{\text{ice}}$ are the specific heat, the thermal conductivity, and the density of ice, respectively; $L_{\text{m}}$ is the latent heat of water solidification. So,

$$\frac{dh}{dt} = \left(\frac{StD}{2t}\right)^{1/2}. \tag{3}$$

Ignoring the slipping phenomena at the ice-water-gas triple line [34], the relationship between $r$ and $h$ can be described as $dr/dh = -1/\tan\varphi$. Combining the geometrical relation that $\tan\varphi = r/(h + R\cos\theta)$ and Eq. (3) gives

$$\frac{dr^2}{dt} = -2\text{St}D - R\cos\theta\left(\frac{2\text{St}D}{t}\right)^{1/2}. \tag{4}$$

With the boundary condition that $t = 0$, $r = b$, $r^2$ is derived as

$$r^2 = -2\text{St}Dt - 2R\cos\theta(2\text{St}Dt)^{1/2} + b^2. \tag{5}$$

Thus, substituting Eqs. (3) and (5) into Eq. (2) yields the bubble formation rate in icing droplets,

$$\frac{dV_{\text{bubble}}}{dt} = \pi\left(1 + \frac{1}{\nu\alpha}\right)^{-1}(-2\text{St}Dt - 2R\cos\theta(2\text{St}Dt)^{1/2} + R^2\sin^2\theta)\left(\frac{\text{St}D}{2t}\right)^{1/2}. \tag{6}$$

Marin *et al.* incidentally captured the bubble formation in freezing droplets using a 2D-like Hele-Shaw setup [9]. Considering the advantages of 2D images for easy processing, we used their experimental results to validate our model. Figures 4(a) and 4(b) show the comparison of ice front height, $h$, and ice front radius, $r$, between the experimental results and the theoretical results. We also validated our model through the comparison of the bubble volume variations in Fig. 4(c). But it should be noted that, since the images by Marin *et al.* are 2D and we can only extract the bubble area

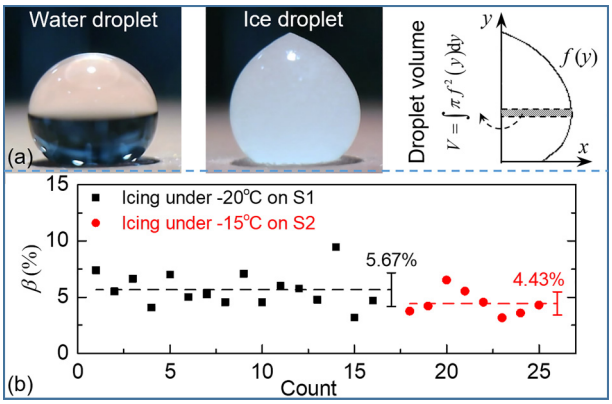


FIG. 5. (a) Calculation method of water droplet volume, $V_{\text{water}}$, and ice droplet volume, $V_{\text{ice}}$. The droplet profiles are extracted first and then integrations are performed along the $y$ axis to get the droplet volumes. The bubble volume fraction in an ice droplet is equal to $1 - V_{\text{water}}/(\nu V_{\text{ice}})$, where $\nu$ is the ratio of ice and water densities. (b) Bubble volume fraction data in ice droplets under different supercooling on surfaces S1 and S2.

from the 2D image, we transformed the 2D bubble area to 3D bubble volume through a mathematical manipulation (see the validation details in the Supplemental Material [29]). As shown in Fig. 4(c), the variations of bubble volume with time from experiments and from our model are consistent, at least in trend. Actually, because of the limitation of current camera technology and the clouding droplet itself, it is impossible to obtain reliable bubble volume variation in a three-dimensional (3D) droplet to validate our model accurately. Even so, the indirect validation results in Fig. 4 support our model. Equation (6) also shows the influencing factors of bubble formation rate, including the air solubility, $\alpha$, the St number (or the supercooled temperature, $\Delta T$), the droplet curvature radius, $R$, the surface CA, $\theta$, as well as the time, $t$. See their detailed influences in the Supplemental Material [29].

For the freezing of supercooled droplets on surfaces S1 and S2, we extracted the profiles of the water droplets and the ice droplets, as shown in Fig. 5(a), and then performed integrations along the $y$ axis to obtain the droplet volumes, $V_{\text{water}}$ and $V_{\text{ice}}$. Thus, the bubble volume fraction in an ice droplet is equal to $1 - V_{\text{water}}/(\nu V_{\text{ice}})$, where $\nu$ is the density ratio of ice and water, which takes a value of 0.92. Figure 5(b) shows the results. The average value of bubble volume fraction in ice droplets on surface S1 is 5.67% with a standard deviation of 1.50% while the value is 4.43 $\pm$ 1.03% for freezing droplets on surface S2. This is because the air solubility in water decreases with increasing water temperature. From the bubble fraction value, we can also infer the air solubility in supercooled water based on the bubble volume conservation that $-20$ °C supercooled water has an air solubility of 6.53 $\pm$ 1.68% and $-15$ °C supercooled water has an air solubility of 5.04 $\pm$ 1.13%. It should be noted that, because the water droplet is not supercooled in the experiments by Marin *et al.*, we used an air solubility of 3% (value at 0 °C) when validating our model in Fig. 4(c).

In summary, we revealed a bubble formation phenomenon in freezing droplets from microscale to millimeter scale. Via a controlled reicing process, we clearly observed the bubbles are dissolved out from the ice front in an icing droplet, and then proposed a theoretical model coupled with the droplet icing physics. Based on the model, the bubble formation rate and its relationship with the main influencing factors (the gas solubility, the supercooled degree, the freezing time, the droplet size, and the surface contact angle) were determined. This work finds that the ice droplet is actually a porous medium rather than complete solid ice, which shall change our previous perception and bring some inspiration to the development of new icing models and the modification of conventional icing calculations. It may also help improve existing anti-icing and deicing techniques.

This work is supported by the National Postdoctoral Program for Innovative Talents (Grant No. BX20180024), the China Postdoctoral Science Foundation (Grant No. 2019M650444), and the National Natural Science Foundation of China (Grant No. 11772034).

[1] M. P. Fuller, A. M. Fuller, S. Kaniouras, J. Christophers, and T. Fredericks, The freezing characteristics of wheat at ear emergence, Eur. J. Agron. **26**, 435 (2007).
[2] F. T. Lynch and A. Khodadoust, Effects of ice accretions on aircraft aerodynamics, Prog. Aerospace Sci. **37**, 669 (2001).
[3] M. R. Nasr, M. Fauchoux, R. W. Besant, and C. J. Simonson, A review of frosting in air-to-air energy exchangers, Renewable Sustainable Energy Rev. **30**, 538 (2014).
[4] S. Jung, M. K. Tiwari, N. V. Doan, and D. Poulikakos, Mechanism of supercooled droplet freezing on surfaces, Nat. Commun. **3**, 615 (2012).
[5] T. M. Schutzius, S. Jung, T. Maitra, P. Eberle, C. Antonini, C. Stamatopoulos, and D. Poulikakos, Physics of icing and rational design of surfaces with extraordinary icephobicity, Langmuir **31**, 4807 (2015).
[6] M. Schremb and C. Tropea, Solidification of supercooled water in the vicinity of a solid wall, Phys. Rev. E **94**, 052804 (2016).
[7] M. Tembely and A. Dolatabadi, A comprehensive model for predicting droplet freezing features on a cold substrate, J. Fluid Mech. **859**, 566 (2018).
[8] X. Zhang, X. Liu, J. Min, and X. Wu, Shape variation and unique tip formation of a sessile water droplet during freezing, Appl. Therm. Eng. **147**, 927 (2019).
[9] A. G. Marin, O. R. Enriquez, P. Brunet, P. Colinet, and J. H. Snoeijer, Universality of Tip Singularity Formation in Freezing Water Drops, Phys. Rev. Lett. **113**, 054301 (2014).
[10] M. F. Ismail and P. R. Waghmare, Universality in freezing of an asymmetric drop, Appl. Phys. Lett. **109**, 234105 (2016).
[11] S. Jung, M. K. Tiwari, and D. Poulikakos, Frost halos from supercooled water droplets, Proc. Natl. Acad. Sci. USA **109**, 16073 (2012).
[12] S. Nath, C. E. Bisbano, P. Yue, and J. B. Boreyko, Duelling dry zones around hygroscopic droplets, J. Fluid Mech. **853**, 601 (2018).
[13] T. M. Schutzius, S. Jung, T. Maitra, G. Graeber, M. Kohme, and D. Poulikakos, Spontaneous droplet trampolining on rigid superhydrophobic surfaces, Nature (London) **527**, 82 (2015).
[14] E. Ghabache, C. Josserand, and T. Seon, Frozen Impacted Drop: From Fragmentation to Hierarchical Crack Patterns, Phys. Rev. Lett. **117**, 074501 (2016).
[15] S. Wildeman, S. Sterl, C. Sun, and D. Lohse, Fast Dynamics of Water Droplets Freezing from the Outside In, Phys. Rev. Lett. **118**, 084101 (2017).
[16] H. J. Cho, D. J. Preston, Y. Zhu, and E. N. Wang, Nanoengineered materials for liquid–vapour phase-change heat transfer, Nat. Rev. Mater. **2**, 16092 (2016).
[17] Y. Hou, M. Yu, Y. Shang, P. Zhou, R. Song, X. Xu, X. Chen, Z. Wang, and S. Yao, Suppressing Ice Nucleation of Supercooled Condensate with Biphilic Topography, Phys. Rev. Lett. **120**, 075902 (2018).
[18] X. Sun and K. Rykaczewski, Suppression of frost nucleation achieved using the nanoengineered integral humidity sink effect, ACS Nano **11**, 906 (2017).
[19] F. Chu, X. Wu, and L. Wang, Dynamic melting of freezing droplets on ultraslippery superhydrophobic surfaces, ACS Appl. Mater. Interfaces **9**, 8420 (2017).
[20] K. Golovin, S. P. Kobaku, D. H. Lee, E. T. DiLoreto, J. M. Mabry, and A. Tuteja, Designing durable icephobic surfaces, Sci. Adv. **2**, e1501496 (2016).
[21] Y. Wang, J. Xue, Q. Wang, Q. Chen, and J. Ding, Verification of icephobic/anti-icing properties of a superhydrophobic surface, ACS Appl. Mater. Interfaces **5**, 3370 (2013).
[22] J. B. Boreyko and C. P. Collier, Delayed frost growth on jumping-drop superhydrophobic surfaces, ACS Nano **7**, 1618 (2013).

[23] F. Chu, D. Wen, and X. Wu, Frost self-removal mechanism during defrosting on vertical superhydrophobic surfaces: Peeling off or jumping off, Langmuir **34**, 14562 (2018).
[24] Q. Zhang, M. He, J. Chen, J. Wang, Y. Song, and L. Jiang, Anti-icing surfaces based on enhanced self-propelled jumping of condensed water microdroplets, Chem. Commun. **49**, 4516 (2013).
[25] A. E. Carte, Air bubbles in ice, Proc. Phys. Soc. **77**, 757 (1961).
[26] J. Hruba and G. Kletetschka, Environmental record of layers of bubbles in natural pond ice, J. Glaciol. **64**, 866 (2018).
[27] C. Madrazo, T. Tsuchiya, H. Sawano, and K. Koyanagi, Air bubbles in ice by simulating freezing phenomenon, J. Soc. Art Sci. **8**, 35 (2009).
[28] Z. Jin, X. Cheng, and Z. Yang, Experimental investigation of the successive freezing processes of water droplets on an ice surface, Int. J. Heat Mass Transfer **107**, 906 (2017).
[29] See Supplemental Material at http://link.aps.org/supplemental/10.1103/PhysRevFluids.4.071601 for supplemental contents and videos S1–S6.
[30] L. Mishchenko, B. Hatton, V. Bahadur, J. A. Taylor, T. Krupenkin, and J. Aizenberg, Design of ice-free nanostructured surfaces based on repulsion of impacting water droplets, ACS Nano **4**, 7699 (2010).
[31] G. G. Stokes, On the effect of internal friction of fluids on the motion of pendulums, Trans. Cambridge Philos. Soc. **9**, 8 (1851).
[32] A. M. Meirmanov, M. Niezgodka, and A. Crowley, *The Stefan problem* (Walter de Gruyter, Berlin, 1992).
[33] V. K. Pinus and P. L. Taylor, Stability and instability in crystal growth: Symmetric solutions of the Stefan problem, Phys. Rev. B **32**, 5362 (1985).
[34] X. Zhang, X. Wu, J. Min, and X. Liu, Modelling of sessile water droplet shape evolution during freezing with consideration of supercooling effect, Appl. Therm. Eng. **125**, 644 (2017).